

Design of antiangiogenic hypoxic cell radiosensitizers: 2-Nitroimidazoles containing a 2-aminomethylene- 4-cyclopentene-1,3-dione moiety

Yoshihiro Uto,^a Hideko Nagasawa,^{a,b} Cheng-Zhe Jin,^a Shinichi Nakayama,^a
Ayako Tanaka,^a Saori Kiyoi,^a Hitomi Nakashima,^a Mariko Shimamura,^c
Seiichi Inayama,^d Tomoya Fujiwara,^e Yoshio Takeuchi,^e Yoshimasa Uehara,^f
Kenneth L. Kirk,^g Eiji Nakata^a and Hitoshi Hori^{a,*}

^aDepartment of Life System, Institute of Technology and Science, Graduate School,
The University of Tokushima, Minamijasanjimacho-2, Tokushima 770-8506, Japan

^bLaboratory of Pharmaceutical Chemistry, Gifu Pharmaceutical University, Mitahorahigashi-5, Gifu 502-8585, Japan

^cMedical Research and Development Center, The Tokyo Metropolitan Institute of Medical Science, 3-18-22 Honkomagome,
Bunkyo-ku, Tokyo 113-8613, Japan

^dInstitute of Oriental Medical Sciences, 2-6-3 Ebisunishi, Shibuya-ku, Tokyo 155-0021, Japan

^eGraduate School of Medicine and Pharmaceutical Sciences for Research, University of Toyama, Sugitani 2630,
Toyama 930-0194, Japan

^fDepartment of Bioactive Molecules, National Institutes of Health, 1-23-1, Shinjuku-ku, Tokyo 162-8640, Japan

^gLaboratory of Bioorganic Chemistry, National Institute of Diabetes and Digestive and Kidney Diseases, National Institutes of Health,
DHHS, Bethesda, MD 20892, USA

Received 21 February 2008; revised 17 April 2008; accepted 19 April 2008

Available online 24 April 2008

Dedicated to the memory of Professor Toshio Satoh of Tokushima Bunri University
who made many lasting contributions to the field of Medicinal Chemistry.

Abstract—We designed chiral 2-nitroimidazole derivatives containing a 2-aminomethylene-4-cyclopentene-1,3-dione moiety as antiangiogenic hypoxic cell radiosensitizers. Based on results of molecular orbital calculations, the 2-aminomethylene-4-cyclopentene-1,3-dione moiety is expected to show high electrophilicity comparable to that of the 2-methylene-4-cyclopentene-1,3-dione moiety included in TX-1123 and tyrphostin AG17. We evaluated the antiangiogenic and radiosensitizing effects of the new compounds, along with other biological properties including their activities as hypoxic cytotoxicities and protein tyrosine kinase (PTK) inhibitory activities. Among the compounds tested, **5** (TX-2036) proved to be the strongest antiangiogenic hypoxic cell radiosensitizer. All the other chiral 2-nitroimidazole derivatives having 2-aminomethylene-4-cyclopentene-1,3-dione moiety tested were also antiangiogenic hypoxic cell radiosensitizers. The PTK inhibitory activity of **5** (TX-2036) showed this to be a promising and potent EGFR kinase inhibitor, having an IC₅₀ value of lower than 2 μM. This compound also was an Flt-1 kinase inhibitor having an IC₅₀ value of lower than 20 μM. Our results show that these chiral 2-nitroimidazole derivatives that contain the 2-aminomethylene-4-cyclopentene-1,3-dione moiety as a potent antiangiogenic pharmacophoric descriptor are promising lead candidates for the development of antiangiogenic hypoxic cell radiosensitizers.

© 2008 Elsevier Ltd. All rights reserved.

1. Introduction

For a neoplastic cell to metastasize, there are a series of steps that it must go through. Each step is rate-limiting in the sense that, until each step is completed, the cell is limited and the subsequent step in the metastatic process

Keywords: Hypoxic cell radiosensitizers; Antiangiogenic agents; 2-Aminomethylene-4-cyclopentene-1,3-dione; Protein tyrosine kinase.

* Corresponding author. Tel.: +81 88 656 7514; fax: +81 88 656 9164; e-mail: hori@bio.tokushima-u.ac.jp

will not occur. Thus, failure to complete any of the steps prevents tumor cells from producing metastasis. Angiogenesis is the first of these rate-limiting steps and angiogenesis is also a prerequisite for neoplastic growth. Since a neoplasm is composed of neoplastic cells, capillary blood vessels, and connective tissue, antiangiogenic agents also can be considered to be antineoplastic agents.¹ Inefficient vascular supply and the resultant hypoxia in tumor tissue often leads to neovascularization to satisfy the needs of surviving tumor tissues. Bevacizumab (Avastin[®]) was the first angiogenesis inhibitor approved by the U.S. Food and Drug Administration (for colon cancer), and the first to demonstrate prolongation of survival in patients with advanced cancer.^{2,3} It is an antivascular endothelial growth factor (VEGF) antibody, and the story of its discovery and manufacture describes a monumental achievement. There are about 200 different types of human cancers, and about 60% of these express VEGF. However, many cancers produce other angiogenic proteins as well. Furthermore, some cancers may initially produce only VEGF but over time can express redundant angiogenic proteins owing to new mutations. At least six angiogenic proteins have been reported for some types of breast cancer. Therefore, in the future, as more patients remain well on bevacizumab therapy, and as bevacizumab receives FDA approval for other tumors, treatment may benefit from co-administration of other antiangiogenic agents as adjuvant therapeutics for tumor growth/regrowth inhibition and antimetastasis.³

Shweiki et al. reported in 1992 that hypoxia induced the production of VEGF, which mediates hypoxia-initiated angiogenesis.⁴ Since this report the link between the tumor tissue hypoxia and angiogenesis gradually became to be established.^{5,6} Since antiangiogenic agent will contribute to hypoxia, it will also benefit the radiotherapy. Based on these considerations, there are apparent advantages to be gained by sensitizing hypoxic cells to radiotherapy while, at the same time, inhibiting angiogenic activity. This combination of the radiosensitizing activity and antiangiogenic activity would be expected to provide a synergistic interaction between the hypoxic cell radiosensitizers and antiangiogenic agents which target hypoxia-initiated neovasculature. Our research has focused on the design and synthesis of compounds that can function as combination drugs containing both radiosensitizing and antiangiogenic activities.

We recently reported the design, synthesis, and evaluation of racemic and enantiomerically pure (chiral) haloacetylcarbamoyl-2-nitroimidazoles, including chloro- and bromo-derivatives, as antiangiogenic hypoxic cell radiosensitizers.⁷ In the tumor microenvironment, there are softer nucleophiles such as non-protein thiols and thiol proteases. Therefore, we developed a strategy to design 2-nitroimidazole derivatives that incorporate a softer electrophile, the aminomethylenecyclopentenedione moiety, as a new antiangiogenic and antitumor functional group. We considered two potential benefits of having a chiral center in our hypoxic cell radiosensitizers: First, this would provide us with two molecular structures expected to exhibit different biological activity

from the same synthetic route and, second, each enantiomer would possess a specific pharmacokinetic property as well as a specific pharmacodynamic property. We present here our design, syntheses, and biological evaluation of new 2-nitroimidazole-based antiangiogenic hypoxic cell radiosensitizers that incorporate the 2-aminomethylene-4-cyclopentene-1,3-dione moiety as an antiangiogenic pharmacophoric descriptor.⁸

2. Results

The goal of this research was to design compounds that would incorporate hypoxic cell radiosensitizing activity and antiangiogenic activity in the molecule through an appropriate linker. The electron deficient 2-nitroimidazole moiety substituted with chiral hydrophobic alkyl- or aryloxy-ethyl groups was chosen to serve the first purpose while the 2-aminomethylene-4-cyclopentene-1,3-dione moiety would function as the latter and also a protein tyrosine kinase (PTK) inhibiting unit, activities previously found by our group. We selected *p*-aminobenzoic acid as the linker between the radiosensitizer unit and antiangiogenic moiety because of its rigidity and its optimum length that permits the design of the molecular structure with a single chiral center possessing greater steric hindrance (Fig. 1).

2.1. Molecular orbital-based molecular modeling

Molecular modeling was used to aid in the design of these new bifunctional 2-nitroimidazole derivatives. We calculated HOMO–LUMO of representative compounds, such as TX-2043 (R = methyl), TX-2030

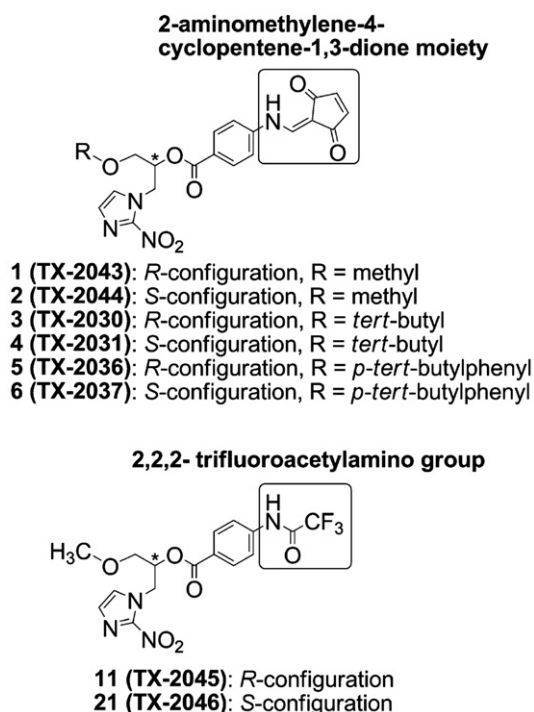


Figure 1. Structure of designed antiangiogenic hypoxic cell radiosensitizers 1–6 and control compounds 11 and 21.

(R = *tert*-butyl), and TX-2036 (R = *p*-*tert*-butylphenyl), and TX-2045 (R = methyl; without cyclopentenedione moiety) as a control of TX-2043 (R = methyl) for a comparison of their MO Eigenvalues and coefficients which are very important factors in MO theory. We first performed geometry and molecular orbital optimizations of the (*R*)-enantiomers of 2-nitroimidazole-aminomethylenecyclopentenediones possessing three different alkyl or aryl groups with different steric demands. These included the methyl group **1** (TX-2043), *tert*-butyl group **3** (TX-2030), and *p*-*tert*-butylphenyl group **5** (TX-2036). The des-aminomethylenecyclopentenedione derivative **11** (TX-2045) was used as a control compound. The molecular orbitals of these compounds that were obtained using the B3LYP hybrid functional and the 6–31G(d) basis set as implemented with the Gaussian program⁹ are shown in Figure 2. These calculations revealed that 2-nitroimidazole-aminomethylenecyclopentenedione such as **1** (TX-2043), **3** (TX-2030), and **5** (TX-2036) have similar LUMO coefficients localized at cyclopentenedione rings indicating that this moiety might be attacked by nucleophiles, especially soft nucleophiles such as thiols present in proteolytic enzymes. In contrast, des-aminomethylenecyclopentenedione **11** (TX-2045) having a trifluoromethyl group instead of cyclopentenedione rings showed LUMO coefficients delocalized in the 4-trifluoroacetylaminobenzoyloxy group.

2.2. Synthesis

The synthetic route used is summarized in Scheme 1. Reaction of 2-nitroimidazole with the enantiomeric alkyl glycidyl ethers produced (*R*)- and (*S*)-2-nitroimidazole-isopropanols (**7–9** and **18–20**) already reported.⁷ Coupling with *p*-trifluoroacetamidobenzoic acid and removal of the trifluoroacetyl group gave the (*R*)- and (*S*)-isopropyl *p*-aminobenzoates (**14–16** and **24–26**). Reaction of isopropyl *p*-aminobenzoates with 2-methoxymethylene-4-cyclopentene-1,3-dione in ethanol produced (*R*)- and (*S*)-2-nitroimidazole-aminomethylenecyclopentenediones (**1, 3, 5** and **2, 4, 6**). The physical data of 2-nitroimidazole-aminomethylenecyclopentenediones are shown in Table 1. The calculated log*P* (Pallas3.0,

CompDrug Chemistry, Ltd) of the proposed radiosensitizers, **1** or **2**, **3** or **4**, and **5** or **6** were 2.55, 3.80, 6.03, respectively, and the calculated log*P* (*c*log*P*) of **11** or **21** and etanidazole were 2.24 and –1.56, respectively.

2.3. Biological activity

Several biological parameters were measured using established assays. We evaluated radiosensitizing activities (EMT6/KU, shown in Table 2), antiangiogenic activities including antitumor or antineoplastic, and antimetastatic activities (proliferation inhibitory activity in EMT6/KU and RLE cells, and inhibitory activities to MMP-2, MMP-9 shown in Table 5, and tyrosine kinases, and in vivo antiangiogenic CAM assay) required for potent antiangiogenic hypoxic cell radiosensitizers.

As shown by enhancement ratios (ERs) shown in Table 2, (1.6 is the minimum effective ER of a radiosensitizer in an in vitro assay) even at a concentration of 1 μM, these new agents have higher radiosensitizing activities than etanidazole (ER = 1.72 at 1 mM) used as a standard radiosensitizer. Interestingly, as shown in Table 3, their antiangiogenesis properties (RLE cell proliferation) showed higher potency (1.3–6.6 times) than their antitumor activities (EMT6/KU cell proliferation). They are potent antiangiogenic hypoxic cell radiosensitizers which function as chemosensitizers to enhance the effects of chemotherapy.

In the chick embryo CAM assay, all new nitroimidazole derivatives showed antiangiogenesis activities and those with the less bulky functional group were the most active (Table 4). They were also effective inhibitors of matrix metalloproteases, as shown for both MMP-2 and MMP-9 (Table 5). Again, the compounds with the less bulky functional groups, and, in particular, the *R*-enantiomers, were the strongest inhibitors (methyl > *tert*-butyl > *p*-*tert*-butylphenyl). Inhibition was greater for MMP-2 than for MMP-9. As expected, the control compounds **11** (TX-2045) and **21** (TX-2046), having the trifluoroacetyl amino group instead of the 2-aminomethylene-4-cyclopentene-1,3-dione moiety, showed weak or no biological activities in the chick embryo CAM and

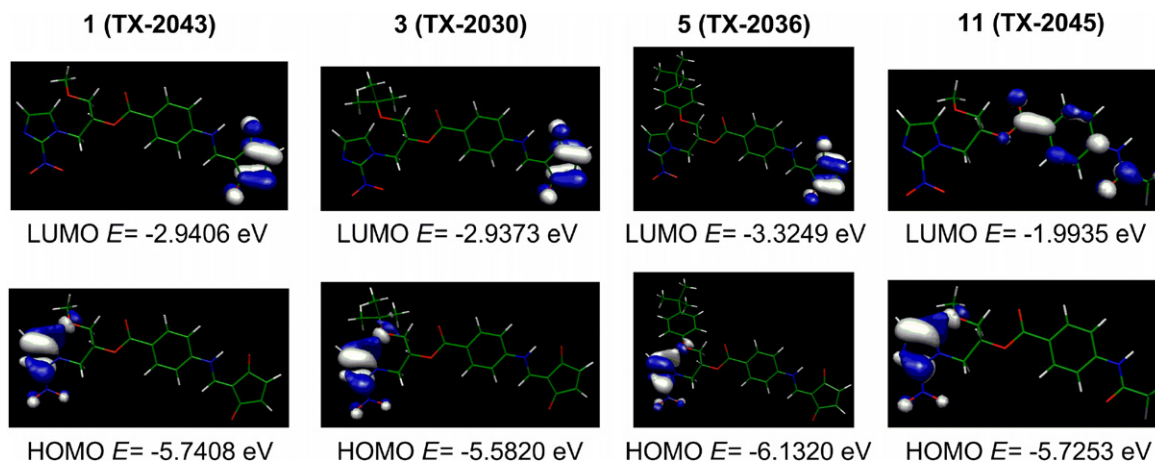


Figure 2. Molecular orbitals of antiangiogenic hypoxic cell radiosensitizers.

MMP assays. With respect to EGFR and Flt-1 inhibition, the methyl and *tert*-butylphenyl group-containing compounds, **1** (TX-2043), **2** (TX-2044), **5** (TX-2036), and **6** (TX-2037), were stronger inhibitors than *tert*-butyl derivatives, **3** (TX-2030) and **4** (TX-2031) (Table 6). This suggests that compounds having less steric encumbrance adjacent to the stereocenter, such as methyl and even *tert*-butylphenyl group, are the stronger inhibitors, and that the bulky *tert*-butyl group reduces activity. Finally, as shown in Table 7, the antitumor activity of **5** (TX-2036) using an in vitro assay of a human cancer cell line panel (HCC panel) consisting of 39 systems suggested reasonable potency as an antiangiogenic hypoxic cell radiosensitizer under aerobic conditions. There were slight, but not significant, eudismic ratios (the potency of the eutomer relative to that of the distomer) for all the biological properties except for tyrosine kinase inhibition where the *R*-enantiomers were stronger inhibitors than *S*-enantiomers.

Based on the results of the several assays, **5** (TX-2036) proved to be the most potent antiangiogenic and antitumor agent among the newly synthesized chiral 2-nitroimidazoles linked to aminomethylenecyclopentenedione.

3. Discussion

Angiogenesis is a fundamental process required for a wide variety of physiological and pathophysiological processes.¹⁰ Angiogenesis provides both a perfusion effect and a paracrine effect to a growing tumor and tumor cells, and endothelial cells can drive each other to perpetuate and amplify the malignant phenotype. A number of antiangiogenic agents have been developed, and many are now in clinical trials. Avastin[®] and a few other drugs have been approved for clinical use. However, before antiangiogenic agents can be successfully incorporated into clinical anticancer strategy, a greater understanding of the process of angiogenesis and of the interaction between the endothelial cell and its tumor microenvironment is required. It had long been assumed that an angiogenesis inhibitor would impair the effect of ionizing radiation by inducing tumor hypoxia. Murata and coworkers¹¹ found that treatment of breast carcinoma xenografts with TNP-470 and fractionated radiotherapy resulted in a decrease in tumor oxygenation and control.

As part of our research to develop clinically effective tumor chemotherapeutics, we developed compounds that combined radiosensitizing activity with antiangiogenic activity. In our previous report, we described our syntheses of the individual enantiomers of haloacetylcarbamoyl-2-nitroimidazole as antiangiogenic hypoxic cell radiosensitizers. The synthetic design allows introduction of diversity in the side-chain ether function, as illustrated by the introduction of methyl, *tert*-butyl, and *p*-*tert*-butylphenyl in this series. The data from biological evaluation suggested that the (*R*)-*p*-*tert*-butylphenyl-bromoacetylcarbamoyl-2-nitroimidazole hypoxic cell radiosensitizer, TX-1898,⁷ may be a very promising candidate for further development as an antiangiogenic

hypoxic cell radiosensitizer. However, the haloacetylcarbamoyl group is a hard electrophile that preferentially reacts with hard nucleophiles.

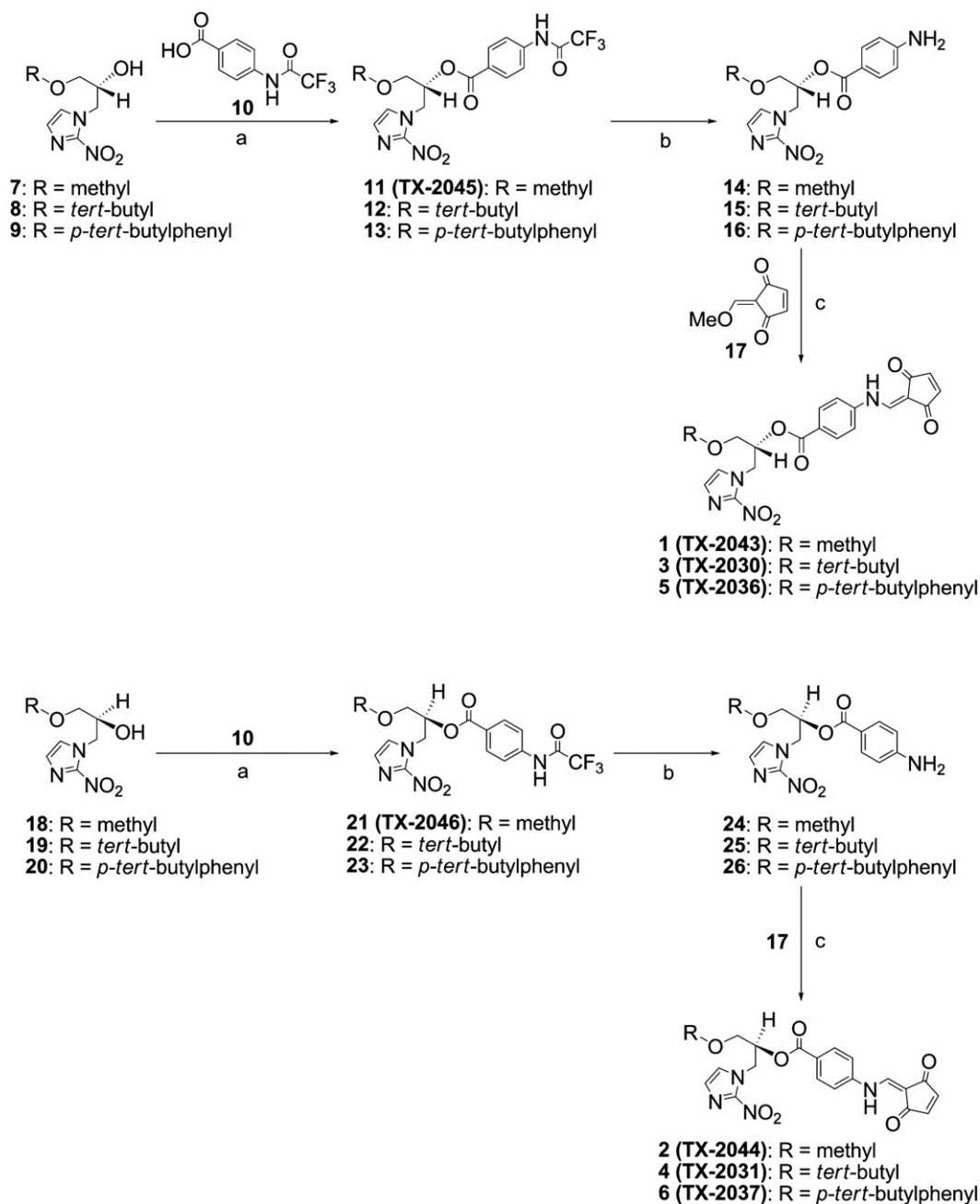
Here, we have prepared new compounds based on a rational design that incorporates a structural unit with known radiosensitizing activity, the chiral 2-nitroimidazole moiety, with functionality designed to have antiangiogenic activity, the 2-aminomethylene-4-cyclopentene-1,3-dione moiety. All of these bifunctional derivatives proved to have activity as antiangiogenic hypoxic cell radiosensitizing agents. We evaluated compound **5** (TX-2036) as the most promising candidate for an antiangiogenic hypoxic cell radiosensitizer overall, based on several factors: (1) Its hypoxic cell radiosensitizing activity is shown in Table 2 (ER = 1.79 at 1 μ M). Potencies are evaluated by the concentration as well as ER values. Thus all the compounds with ER of more than 1.6 at 1 μ M showed similar potency. (2) Its potent EGFR kinase inhibitory activity (IC₅₀ = 1.8 μ M) is shown in Table 6. This potent activity attracted our attention because of the important role of EGFR (epidermal growth factor receptor) tyrosine kinases as regulators of angiogenesis, proliferation, migration, tumorigenesis, and metastasis. (3) Its antiproliferatory activity (IC₅₀ = 0.81 μ M) to RLE cells is shown in Table 3. (4) Its in vivo antiangiogenic activity using a CAM assay (the inhibition of 64% at 1 μ g per CAM) shown in Table 4. The potencies are evaluated by the dose per CAM as well as the inhibition rate. Thus, all the compounds with an inhibition of more than 60% at the same concentration are evaluated as being similar potent. (5) Its moderate MMPs inhibitory activity, being the second most potent among the compounds tested, having similar potency to MMP-2 and MMP-9 (IC₅₀ = 77 μ M and IC₅₀ = 67 μ M).

In conclusion, **5** (TX-2036) has activities that suggest it is a very promising candidate for further development as an antiangiogenic hypoxic cell radiosensitizer.

4. Experimental

4.1. General procedures

¹H NMR spectra were recorded on a JEOL JNM-EX400 spectrometer (400 MHz) with tetramethylsilane as the internal standard. Chemical shifts are reported in ppm. Coupling constants are reported in Hz. IR spectra were measured in KBr pellets with a Perkin-Elmer 1600 spectrometer. Mass spectra were measured on a Shimadzu GC-MS QP-1000 mass spectrometer using EI method. Reaction was monitored by analytical thin-layer chromatography (TLC) using Merck silica gel 60 F₂₅₄ glass plates and Merck aluminum oxide 60 F₂₅₄ neutral plates (Type E). Column chromatography was performed on Merck silica gel 60 (230–400 mesh) and aluminum oxide 90 active neutral (70–230 mesh). Optical rotations were determined on a JASCO DIP-370 digital polarimeter. All melting points were measured with a micromelting point apparatus (MP-S3 model) and are uncorrected. Elemental analyses were performed with a



Scheme 1. Synthesis of antiangiogenic hypoxic cell radiosensitizers **1–6**. Reagents and conditions: (a) 4-DMAP, DIPC/CH₃CN; (b) NaBH₄/EtOH, rt; (c) EtOH, reflux.

Yanako CHN Corder MT-5. All chemicals were purchased from Wako Pure Chemical Industries, Ltd (Osaka, Japan), Kanto Chemical Co. Inc., (Tokyo, Japan), Tokyo Chemical Industry Co., Ltd (Tokyo, Japan), and Sigma–Aldrich Japan (Tokyo, Japan). (*S*)-(+)-Epiclorohydrin (99.9% pure, 98.9% ee) and (*R*)-(–)-epiclorohydrin (99.6% pure, 98.6% ee) were provided by DAISO Co., Ltd (Osaka, Japan).

Table 1. Physical data of chiral 2-nitroimidazole-aminomethylene-cyclopentenediones

Drugs	Absolute configuration	R	<i>c</i> log <i>P</i>	Mp (°C)
1 (TX-2043)	<i>R</i>	Me	2.55	149–150
2 (TX-2044)	<i>S</i>	Me		146–147
3 (TX-2030)	<i>R</i>	<i>tert</i> -Bu	3.80	131–132
4 (TX-2031)	<i>S</i>	<i>tert</i> -Bu		130–131
5 (TX-2036)	<i>R</i>	<i>p</i> - <i>tert</i> -BuPh	6.03	186–188
6 (TX-2037)	<i>S</i>	<i>p</i> - <i>tert</i> -BuPh		187–188

ka, Japan), Kanto Chemical Co. Inc., (Tokyo, Japan), Tokyo Chemical Industry Co., Ltd (Tokyo, Japan), and Sigma–Aldrich Japan (Tokyo, Japan). (*S*)-(+)-Epiclorohydrin (99.9% pure, 98.9% ee) and (*R*)-(–)-epiclorohydrin (99.6% pure, 98.6% ee) were provided by DAISO Co., Ltd (Osaka, Japan).

4.2. Molecular modeling methods

The molecular geometries were calculated with a B3LYP hybrid density functional in conjunction with the 3-21G(d) basis set using the GAUSSIAN 98 suite of programs.⁹ Using their molecular geometries obtained above, their molecular orbital calculations were per-

Table 2. Radiosensitizing activity of 2-nitroimidazole-aminomethylene-cyclopentenediones

Compounds	ER (concn)
Etanidazole	1.72 (1 mM)
1 (TX-2043)	1.80 (1 μ M)
2 (TX-2044)	2.00 (1 μ M)
3 (TX-2030)	1.68 (1 μ M)
4 (TX-2031)	1.80 (1 μ M)
5 (TX-2036)	1.79 (1 μ M)
6 (TX-2037)	1.93 (1 μ M)
11 (TX-2045)	2.02 (1 μ M)
21 (TX-2046)	1.84 (1 μ M)

ER (concn): enhancement ratio at corresponding concentration.

Table 3. Proliferation inhibitory activities of chiral 2-nitroimidazole-aminomethylenecyclopentenediones in the EMT6/KU cells and RLE cells

Drugs	IC ₅₀ (μ M)	
	EMT6/KU	RLE
1 (TX-2043)	5.50	1.14
2 (TX-2044)	10.92	2.28
3 (TX-2030)	7.04	1.23
4 (TX-2031)	2.67	2.13
5 (TX-2036)	5.32	0.81
6 (TX-2037)	3.96	0.77
TX-1123	—	0.82
AG17	—	8.27

formed with the B3LYP hybrid density functional in conjugation with the 6-31G(d) basis set in the same programs.

4.3. Synthesis

4.3.1. Synthesis of 4-(trifluoroacetyl-amido)benzoic acid (10). Trifluoroacetic anhydride (3 mL) was added dropwise to a solution of 4-aminobenzoic acid (1.371 g, 10 mmol) in 10 mL of neat trifluoroacetic acid cooled to 0 °C. After the mixture was stirred for 1 h, a precipitate slowly formed. The reaction was checked for completion and more trifluoroacetic anhydride was added if required. Upon completion, the reaction mixture was poured over crushed ice (300 mL) whereupon a voluminous white precipitate formed. After 1 h, the solid was filtered, washed with copious amounts of water, and allowed to air dry at 50–60 °C for 12 h to afford 4-(trifluoroacetyl-amido)benzoic acid **10** as a white solid (2.25 g, yield: 96.6%). Mp 154–156 °C (sublimed); IR (KBr; cm⁻¹): 3326 (NH), 3198–2376 (br, COOH), 1712 (CO), 1680 (COOH), 1541, 1290, 1189 (s); ¹H NMR (C₂D₆SO) δ 11.51 (s, 1H), 7.98 (d, *J* = 7.6 Hz, 2H), 7.81 (d, *J* = 7.9 Hz, 2H). Anal. Calcd for C₉H₆NO₃: C, 46.36; H, 2.59; N, 6.01. Found: C, 46.32; H, 2.77; N, 6.24.

4.3.2. Synthesis of 2-methoxymethylene-4-cyclopentene-1,3-dione (17). A mixture of 4-cyclopentene-1,3-dione (95%, 1.406 g, 13.9 mmol), trimethylorthoformate (7.970 g, 75 mmol), zinc chloride (436.8 mg, 3 mmol), and acetic anhydride (30 mL, ca. 300 mmol) was refluxed for 6 h. The reaction mixture was cooled to room temperature, concentrated in vacuo to remove acetic anhydride, and the residue was separated by silica gel chromatography (silica gel N60; 40–50 μ m; ethyl acetate/*n*-hexane, 1:1) to afford 1.01 g (52%) of 2-methoxymethylene-4-cyclopentene-1,3-dione.

Table 4. Antiangiogenic activities of 2-nitroimidazole-aminomethylenecyclopentenediones using a CAM assay

Compounds	Configuration	R	Inhibition %			
			100 μ g/CAM	5 μ g/CAM	1 μ g/CAM	100 ng/CAM
1 (TX-2043)	<i>R</i>	Me	ND	80	71	60
2 (TX-2044)	<i>S</i>	Me	ND	80	53	25
3 (TX-2030)	<i>R</i>	<i>tert</i> -Bu	ND	50	50	ND
4 (TX-2031)	<i>S</i>	<i>tert</i> -Bu	ND	100	77	ND
5 (TX-2036)	<i>R</i>	<i>p-tert</i> -BuPh	ND	38	64	ND
6 (TX-2037)	<i>S</i>	<i>p-tert</i> -BuPh	ND	57	46	ND
11 (TX-2045)	<i>R</i>		43	ND	ND	ND
21 (TX-2046)	<i>S</i>		83	ND	ND	ND

Table 5. MMP-2 and MMP-9 inhibitory activities (IC₅₀/ μ M)

	1 (TX-2043)	2 (TX-2044)	3 (TX-2030)	4 (TX-2031)	5 (TX-2036)	6 (TX-2037)	11 (TX-2045)	21 (TX-2046)
MMP-2	24	ND	49	50	77	183	>240	>240
MMP-9	53	ND	102	128	67	103	>240	>240

Table 6. Tyrosine kinase inhibitory activities (IC₅₀/ μ M)

	1 (TX-2043)	2 (TX-2044)	3 (TX-2030)	4 (TX-2031)	5 (TX-2036)	6 (TX-2037)
EGFR	2.3	23	21.3	213	1.8	18.4
Flt-1	23.4	ND	21.3	213	18.4	184

Table 7. Antitumor screening data of **5** (TX-2036) on HCC panel

Cell	GI ₅₀ (μM)	TGI (μM)	LC ₅₀ (μM)
<i>Breast</i>			
HBC-4	15	41	>100
BSY-1	13	29	66
HBC-5	2.2	72	68
MCF7	22	63	>100
MDA-MB-231	12	29	68
<i>CNS</i>			
U251	17	33	63
SF-268	24	52	>100
SF-295	21	39	73
SF-539	20	45	>100
SNB-75	18	38	77
SNB-78	18	44	>100
<i>Colon</i>			
HCC2998	17	36	77
KM-12	16	32	67
HT-29	13	34	87
HCT-15	21	42	84
HCT-116	16	34	73
<i>Lung</i>			
NCI-H23	18	42	>100
NCH-H226	20	51	>100
NCI-H522	11	33	98
NCI-H460	18	43	>100
A549	19	39	83
DMS273	12	29	70
DMS114	16	35	73
<i>Melanoma</i>			
LOX-IMVI	18	35	82
<i>Ovarian</i>			
OVCAR-3	18	57	>100
OVCAR-4	22	51	>100
OVCAR-5	14	27	55
OVCAR-8	20	45	99
SK-OV-3	18	33	60
<i>Renal</i>			
RXF-631L	18	34	64
ACHN	17	31	57
<i>Stomach</i>			
St-4	20	48	>100
MKN1	3	13	>100
MKN7	19	42	97
MKN128	19	42	95
MKN45	19	37	74
MKN74	18	39	87
<i>Prostate</i>			
DU-145	18	33	63
PC-3	17	36	76

oxymethylene-4-cyclopentene-1,3-dione **17** as yellow solids. IR (KBr; cm⁻¹): 1728 (s, C=O); 1675 (s), 1637 (s, C=C); 1295, 1135 (s, Me-O), 692 (s, H-C=C-H). ¹H NMR (CD₃OD): δ 3.30–3.32 (m, 3H, O-CH₃), 3.33–3.38 (m, 1H, =CH(OCH₃)), 7.06 and 7.45 (dd, 1H, H-C=C). Anal. Calcd for C₇H₆O₃: C, 60.87; H, 4.38. Found: C, 60.85; H, 4.47.

4.3.3. Synthesis of 1 (TX-2043). Diisopropylcarbodiimide (757.2 mg/930 μL, 6.0 mmol) was added to a solution of (2*R*)-3-methoxy-1-(2-nitroimidazolyl)-2-pro-

panol **7**⁷ (603 mg, 3.0 mmol), **10** (1.399 g, 6.0 mmol), and 4-dimethylaminopyridine (36.7 mg, 0.3 mmol) in acetonitrile (30 mL). The mixture was stirred under nitrogen at 35–40 °C for 24 h and was cooled, filtered, and the filtrate was evaporated to dryness. The crude product mixture was dissolved in CH₂Cl₂, washed with 5% sodium bicarbonate and brine, dried (Na₂SO₄), and concentrated in vacuo. The residue was separated by silica gel column chromatography (ethyl acetate/*n*-hexane, 2:3) to give 723 mg (57.9%) of (2*R*)-3-methoxy-1-(2-nitroimidazolyl)-2-propyl-4'-(trifluoroacetamido)benzoate, **11** (TX-2045). Mp 179–180 °C; IR (KBr; cm⁻¹): 3262, 2942, 1717, 1605, 1544, 1498, 1376, 1250, 1205, 1151, 1098, 845, 769, 734; ¹H NMR (C₂D₆SO): δ 11.56 (s, 1H), 7.92 (d, *J* = 8.8 Hz, 2H), 7.82 (d, *J* = 8.4 Hz, 2H), 7.66 (s, 1H), 7.08 (s, 1H), 5.58 (m, 1H), 4.88 (dd, *J* = 14.4 Hz, 1H), 4.69 (dd, *J* = 14.4 Hz, 1H), 3.69 (dd, *J* = 11.6 Hz, 2H), 3.37 (s, 3H). Anal. Calcd for C₁₆H₁₅F₃N₄O₆: C, 46.16; H, 3.63; N, 13.46. Found: C, 46.55; H, 3.78; N, 13.58.

To a solution of **11** (249.8 mg, 0.6 mmol) in 10 mL of absolute ethanol was added 27.2 mg (0.72 mmol) of sodium borohydride and the reaction was stirred overnight at room temperature. The reaction mixture was quenched by the addition of water (20 mL) and the volatile solvent was removed in vacuo. The remaining aqueous solution was then extracted with ethyl acetate and the organic layer was washed with brine, dried (Na₂SO₄), and concentrated in vacuo. The crude product was purified by flash chromatography to afford (2*R*)-3-methoxy-1-(2-nitroimidazolyl)-2-propyl-4'-aminobenzoate **14** (119.6 mg, 59.3%). Mp 115–116 °C; IR (KBr; cm⁻¹): 3337, 3220, 1690, 1602, 1518, 1485, 1363, 1269, 1173, 1109, 839, 767, 700; ¹H NMR (400 MHz, C₂D₆SO): δ 7.60 (s, 1H), 7.54 (d, *J* = 8.4 Hz, 2H), 7.08 (s, 1H), 6.53 (d, *J* = 8.4 Hz, 2H), 6.0 (s, 2H), 5.47 (m, 1H), 4.83 (dd, *J* = 14.4 Hz, 1H), 4.66 (dd, *J* = 14.0 Hz, 1H), 3.62 (dd, *J* = 10.8 Hz, 2H), 3.37 (s, 3H). Anal. Calcd for C₁₄H₁₆N₄O₅: C, 52.50; H, 5.03; N, 17.49. Found: C, 52.55; H, 4.95; N, 17.32.

A mixture of **14** (119.6 mg, 0.36 mmol), **17** (60.8 mg, 0.44 mmol), and EtOH (10 mL) was refluxed for 5 h and the resulting mixture was evaporated under aspirator vacuum. The residue was purified by silica gel column chromatography (silica gel 60 N, hexane/ethyl acetate, 3:2) to give yellow crystals of **1** (TX-2043, 148.6 mg, 96.8%). Mp 149–150 °C; [α]_D²⁶ +148.0° (*c* 1.0, CHCl₃); IR (KBr; cm⁻¹): 3423, 2931, 1719, 1655, 1603, 1583, 1490, 1365, 1266, 1205, 1181, 1106, 847, 764, 687; ¹H NMR (CDCl₃): δ 10.2 (d, *J* = 13.2 Hz, 1H), 7.98 (d, *J* = 8.8 Hz, 2H), 7.96 (s, 1H), 7.20 (d, *J* = 8.8 Hz, 2H), 7.09 (d, *J* = 2.0 Hz, 2H), 6.95 (dd, *J* = 6.0 Hz, 2H), 5.58 (m, 1H), 4.99 (dd, *J* = 14.4 Hz, 1H), 4.73 (dd, *J* = 14.4 Hz, 1H), 3.64 (dd, *J* = 10.8 Hz, 2H), 3.42 (s, 3H). Anal. Calcd for C₂₀H₁₈N₄O₇: C, 56.34; H, 4.26; N, 13.14. Found: C, 56.09; H, 4.33; N, 12.98.

4.3.4. Synthesis of 2 (TX-2044). Diisopropylcarbodiimide (378.6 mg/465 μL, 3.0 mmol) was added to a solution of (2*S*)-3-methoxy-1-(2-nitroimidazolyl)-2-pro-

panol **18**⁷ (301.7 mg, 1.5 mmol), **10** (653.4 mg, 2.8 mmol), and 4-dimethylaminopyridine (18.33 mg, 0.15 mmol) in 10 mL of acetonitrile. The mixture was stirred under nitrogen at 35–40 °C for 24 h. After this time the mixture was cooled, filtered, and the filtrate was evaporated to dryness. The crude reaction mixture was then dissolved in CH₂Cl₂, washed with 5% sodium bicarbonate and brine, dried (Na₂SO₄), and concentrated in vacuo. The crude mixture was separated by silica gel column chromatography (ethyl acetate/hexane, 2:3) to give (2*S*)-3-methoxy-1-(2-nitroimidazolyl)-2-propyl-4'-(trifluoroacetamido)benzoate, **21** (TX-2046, 285 mg, 45.7%). Mp 177–178 °C; IR (KBr; cm⁻¹): 3262, 2942, 1717, 1605, 1544, 1498, 1376, 1250, 1205, 1151, 1098, 845, 769, 734; ¹H NMR (C₂D₆SO): δ 11.56 (s, 1H), 7.92 (d, *J* = 8.8 Hz, 2H), 7.82 (d, *J* = 8.4 Hz, 2H), 7.66 (s, 1H), 7.08 (s, 1H), 5.58 (m, 1H), 4.88 (dd, *J* = 14.4 Hz, 1H), 4.69 (dd, *J* = 14.4 Hz, 1H), 3.69 (dd, *J* = 11.6 Hz, 2H), 3.37 (s, 3H). Anal. Calcd for C₁₆H₁₅F₃N₄O₆: C, 46.16; H, 3.63; N, 13.46. Found: C, 46.14; H, 3.89; N, 13.21.

To a solution of **21** (249 mg, 0.6 mmol) in 10 mL of absolute ethanol was added 43.2 mg (1.2 mmol) of sodium borohydride and the mixture was stirred overnight at room temperature. The reaction mixture was quenched by the addition of water (20 mL) and the volatile solvent was removed in vacuo. The remaining aqueous solution was extracted with ethyl acetate and the organic layer was washed with brine, dried (Na₂SO₄), and concentrated in vacuo. The residue of crude product was purified by flash chromatography to afford (2*S*)-3-methoxy-1-(2-nitroimidazolyl)-2-propyl-4'-aminobenzoate **24** (184 mg, yield: 91.2%). Mp 115–116 °C; IR (KBr; cm⁻¹): 3337, 3220, 1690, 1602, 1518, 1485, 1363, 1269, 1173, 1109, 839, 767, 700; ¹H NMR (400 MHz, C₂D₆SO): δ 7.60 (s, 1H), 7.54 (d, *J* = 8.4 Hz, 2H), 7.08 (s, 1H), 6.53 (d, *J* = 8.4 Hz, 2H), 6.0 (s, 2H), 5.47 (m, 1H), 4.83 (dd, *J* = 14.4 Hz, 1H), 4.66 (dd, *J* = 14.0 Hz, 1H), 3.62 (dd, *J* = 10.8 Hz, 2H), 3.37 (s, 3H).

A mixture of **24** (148 mg, 0.44 mmol), **17** (72.9 mg, 0.53 mmol), and EtOH (15 mL) was refluxed for 5 h, and then cooled and concentrated under aspirator vacuum. The residue was separated by silica gel column chromatography (silica gel 60 N, hexane/ethyl acetate, 3:2) to give 103 mg, (54.9%) of **2** (TX-2044) as yellow crystals. Mp 146–147 °C; [α]_D²⁶ -151.0° (*c* 1.0, CHCl₃); IR (KBr; cm⁻¹): 3337, 2974, 1717, 1664, 1621, 1573, 1461, 1365, 1253, 1167, 841, 767; ¹H NMR (CDCl₃): δ 10.2 (d, *J* = 12.8 Hz, 1H), 7.97 (d, *J* = 8.4 Hz, 2H), 7.93 (s, 1H), 7.19 (d, *J* = 8.4 Hz, 2H), 7.18 (s, 1H), 7.09 (s, 1H), 6.94 (dd, *J* = 6.0 Hz, 2H), 5.58 (m, 1H), 4.99 (dd, *J* = 14.0 Hz, 1H), 4.73 (dd, *J* = 14.4 Hz, 1H), 3.64 (dd, *J* = 13.6 Hz, 2H), 3.42 (s, 3H). Anal. Calcd for C₂₀H₁₈N₄O₇: C, 56.34; H, 4.26; N, 13.14. Found: C, 56.35; H, 4.50; N, 12.87.

4.3.5. Synthesis of 3 (TX-2030). Diisopropylcarbodiimide (126 mg/153 μL, 1 mmol) was added to a solution of (2*R*)-3-*tert*-butoxy-1-(2-nitroimidazolyl)-2-propanol **8**⁷ (121.63 mg, 0.5 mmol), **10** (233.1 mg, 1 mmol), and

4-dimethylaminopyridine (6.109 mg, 0.05 mmol) in acetonitrile (5 mL). After the mixture was stirred at 40–50 °C for 24 h under a nitrogen atmosphere, it was cooled, filtered, and the filtrate was evaporated to dryness. The crude product mixture was dissolved in CH₂Cl₂, washed with 5% sodium bicarbonate and brine, dried (Na₂SO₄), and concentrated in vacuo to give 387 mg of crude (2*R*)-3-*tert*-butoxy-1-(2-nitroimidazolyl)-2-propyl-4'-(trifluoroacetamido)benzoate **12**. This was suspended in absolute ethanol (10 mL) and sodium borohydride (90%, 43.8 mg, 1 mmol) was added. The mixture was stirred in a 36–46 °C water bath for 4 h, cooled, and then quenched by dropwise addition of 5 mL of water. The volatile solvent was removed in vacuo and the remaining aqueous solution was extracted with ethyl acetate. The organic layer was washed with brine, dried (Na₂SO₄), and concentrated in vacuo to give the crude product which was purified by flash chromatography. This afforded 144.8 mg (79.9%) of (2*R*)-3-*tert*-butoxy-1-(2-nitroimidazolyl)-2-propyl-4'-aminobenzoate **15**. IR (KBr; cm⁻¹): 3342 (NH₂), 2974, 1701 (CO), 1624, 1605, 1365 (imidazolyl-NO₂), 1266, 1170, 1103, 839, 769, 697; ¹H NMR (C₂D₆SO): δ 1.55 (s, 1H), 7.92 (d, *J* = 8.4 Hz, 2H), 7.82 (d, *J* = 8.8 Hz, 2H), 7.66 (s, 1H), 7.08 (s, 1H), 5.46 (m, 1H), 4.90 (dd, *J* = 7.2 Hz, 1H), 4.65 (dd, *J* = 9.2 Hz, 1H), 3.65 (dd, *J* = 7.4 Hz, 2H), 1.19 (s, 9H). MS (EI) *m/z*: 362 (M⁺).

A solution of **15** (217.1 mg, 0.60 mmol) and **17** (100 mg, 0.72 mmol) in 10 mL of EtOH was refluxed for 24 h. The mixture was concentrated under aspirator vacuum and the residue was purified by silica gel column chromatography (silica gel 60 N, hexane/ethyl acetate, 3:2) to give 248.6 mg (88.4%) of **3** (TX-2030) as a yellow crystals. Mp 131–132 °C; [α]_D²⁶ +137.2° (*c* 0.61, CHCl₃); IR (KBr; cm⁻¹): 3340, 2971, 1718, 1659, 1603, 1491, 1365, 1266, 1103, 847, 767; ¹H NMR (C₂D₆SO): δ 10.6 (d, 1H), 8.04 (d, *J* = 13.2 Hz, 1H), 7.86 (d, *J* = 8.8 Hz, 2H), 7.64 (d, *J* = 9.2 Hz, 3H), 7.15 (d, *J* = 5.9 Hz, 1H), 7.09 (d, *J* = 6.8 Hz, 2H), 5.44 (m, 1H), 4.87 (dd, *J* = 13.9 Hz, 1H), 4.65 (dd, *J* = 14.4 Hz, 1H), 3.63 (dd, *J* = 12.8 Hz, 2H), 1.18 (s, 9H). Anal. Calcd for C₂₃H₂₄N₄O₇: C, 58.97; H, 5.16; N, 11.96. Found: C, 58.69; H, 5.40; N, 11.85.

4.3.6. Synthesis of 4 (TX-2031). Diisopropylcarbodiimide (126.20 mg/153 μL, 1 mmol) was added to a solution of (2*S*)-3-*tert*-butoxy-1-(2-nitroimidazolyl)-2-propanol **19**⁷ (121.63 mg, 0.5 mmol), **10** (233.14 mg, 1 mmol), and 4-dimethylaminopyridine (6.109 mg, 0.05 mmol) in 5 mL of acetonitrile. The mixture was stirred under nitrogen at 40–50 °C for 24 h and was then cooled, filtered, and the filtrate was evaporated to dryness. The crude product mixture was dissolved in CH₂Cl₂, washed with 5% sodium bicarbonate and brine, dried (Na₂SO₄), and concentrated in vacuo to give crude (2*S*)-3-*tert*-butoxy-1-(2-nitroimidazolyl)-2-propyl-4'-(trifluoroacetamido)benzoate **22** (189.1 mg, 82.5%). This was suspended in absolute ethanol (10 mL), sodium borohydride (90%, 43.8 mg, 1 mmol) was added, and the mixture was stirred at 36–46 °C for 4 h. The reaction mixture was cooled and quenched by the dropwise addition of water (5 mL) and the volatile solvent was removed in va-

cuo. The remaining aqueous solution was extracted with ethyl acetate and the organic layer washed with brine, dried (Na_2SO_4), and concentrated in vacuo. The residue was purified by flash chromatography to afford (2*S*)-3-*tert*-butoxy-1-(2-nitroimidazolyl)-2-propyl-4'-aminobenzoate **25** (113 mg, 79.4%). IR (KBr; cm^{-1}): 3337 (NH_2), 2963, 1701 (CO), 1605, 1541, 1483, 1365 (imidazolyl- NO_2), 1263, 1173, 1098, 804, 767. ^1H NMR ($\text{C}_2\text{D}_6\text{SO}$): δ 11.55 (s, 1H), 7.92 (d, $J = 8.4$ Hz, 2H), 7.82 (d, $J = 8.8$ Hz, 2H), 7.66 (s, 1H), 7.08 (s, 1H), 5.46 (m, 1H), 4.90 (dd, $J = 7.2$ Hz, 1H), 4.65 (dd, $J = 9.2$ Hz, 1H), 3.65 (dd, $J = 7.4$ Hz, 2H), 1.19 (s, 9H). MS (EI) m/z : 362 (M^+).

A mixture of **25** (51.85 mg, 0.14 mmol), **17** (20.72 mg, 0.15 mmol), and EtOH (5 mL) was refluxed for 24 h. After removal of solvents under aspirator vacuum, the residue was purified by silica gel column chromatography (silica gel 60 N, hexane/ethyl acetate, 3:2) to give 44.6 mg (66.6%) of **4** (TX-2031) as yellow crystals, Mp 130–131 °C. $[\alpha]_{\text{D}}^{26} -141.0^\circ$ (c 0.63, CHCl_3); IR (KBr; cm^{-1}): 3323, 2974, 1717, 1659, 1603, 1541, 1488, 1365, 1269, 1183, 1103, 847, 767; ^1H NMR ($\text{C}_2\text{D}_6\text{SO}$): δ 10.6 (d, 1H), 8.04 (d, $J = 13.2$ Hz, 1H), 7.86 (d, $J = 8.8$ Hz, 2H), 7.64 (d, $J = 9.2$ Hz, 3H), 7.15 (d, $J = 5.9$ Hz, 1H), 7.09 (d, $J = 6.8$ Hz, 3H), 5.44 (m, 1H), 4.87 (dd, $J = 13.9$ Hz, 1H), 4.65 (dd, $J = 14.4$ Hz, 1H), 3.63 (dd, $J = 12.8$ Hz, 2H), 1.18 (s, 9H). Anal. Calcd for $\text{C}_{23}\text{H}_{24}\text{N}_4\text{O}_7$: C, 58.97; H, 5.16; N, 11.96. Found: C, 58.75; H, 5.36; N, 11.74.

4.3.7. Synthesis of 5 (TX-2036). To a solution of (2*R*)-*p*-*tert*-butylphenoxy-1-(2-nitroimidazolyl)-2-propanol **9**⁷ (159.7 mg, 0.5 mmol), **10** (239 mg, 1 mmol), and 4-dimethylaminopyridine (14.2 mg, 0.08 mmol) in acetonitrile (5 mL) was added diisopropylcarbodiimide (ca. 164 mg/200 μL , 1.3 mmol) and the mixture was stirred under nitrogen at 35–45 °C for 24 h. After this time the mixture was cooled, filtered, and the filtrate was evaporated to dryness. The crude product mixture was dissolved in CH_2Cl_2 , washed with 5% sodium bicarbonate and brine, dried (Na_2SO_4), and concentrated in vacuo. The crude product was purified by flash chromatography (ethyl acetate ester/hexane, 2:3) to afford (2*R*)-3-*p*-*tert*-butylphenoxy-1-(2-nitroimidazolyl)-2-propyl-4'-(trifluoroacetamido)benzoate **13** (179.7 mg, yield: 74.7%), Mp 180–181 °C.

Sodium borohydride (36.8 mg, 1.0 mmol) was added to a solution of **13** (158.8 mg, 0.297 mmol) in 10 mL of absolute ethanol, and the mixture was stirred overnight at room temperature. The solution was then cooled and quenched by the dropwise addition of water (5 mL). After removal of the volatile solvent in vacuo, the remaining aqueous solution was extracted with ethyl acetate and the organic layer washed with brine, dried (Na_2SO_4), and concentrated in vacuo. The residue of crude product was purified by flash chromatography to afford (2*R*)-*p*-*tert*-butylphenoxy-1-(2-nitroimidazolyl)-2-propyl-4'-aminobenzoate, **16** (114.2 mg, 87.7%). IR (KBr; cm^{-1}): 3337, 2963, 1701, 1603, 1515, 1490, 1365, 1245, 1170, 1101, 836, 769, 700; ^1H NMR ($\text{C}_2\text{D}_6\text{SO}$): δ 11.55 (s, 1H), 7.92 (d, $J = 8.4$ Hz, 2H),

7.82 (d, $J = 8.8$ Hz, 2H), 7.66 (s, 1H), 7.08 (s, 1H), 5.46 (m, 1H), 4.90 (dd, $J = 7.2$ Hz, 1H), 4.65 (dd, $J = 9.2$ Hz, 1H), 3.65 (dd, $J = 7.4$ Hz, 2H), 1.19 (s, 9H). MS (EI) m/z : 438 (M^+).

A mixture of **16** (100 mg, 0.23 mmol), **17** (37.29 mg, 0.27 mmol), and EtOH (10 mL) was refluxed for 24 h. The product mixture was then evaporated under aspirator vacuum and the residue was purified by silica gel column chromatography (silica gel 60 N, hexane/ethyl acetate, 3:2) to give **5** (34 mg, 27.4%) (TX-2036) as a yellow crystals. Mp 186–188 °C; $[\alpha]_{\text{D}}^{26} +63.3^\circ$ (c 0.40, CHCl_3), IR (KBr; cm^{-1}): 3337, 2963, 1717, 1659, 1605, 1488, 1365, 1263, 1103, 847, 767, 687; ^1H NMR ($\text{C}_2\text{D}_6\text{SO}$): δ 10.6 (d, $J = 13.6$ Hz, 1H: NH), 8.03 (d, $J = 13.6$ Hz, 1H: N-CH=), 7.85 (d, $J = 8.5$ Hz, 2H), 7.69 (s, 1H: imidazole), 7.64 (d, $J = 8.8$ Hz, 2H), 7.29 (d, $J = 8.8$ Hz, 2H), 7.16 and 7.08 (each d, $J = 6.0$, 6.4 Hz, each 1H), 7.10 (d, $J = 0.8$ Hz, 1H), 6.91 (d, $J = 8.8$ Hz, 2H), 5.77 (m, 1H), 5.01 (d, $J = 12.4$ Hz, 1H), 4.84 (dd, $J = 9.2$ Hz, 1H), 4.36 (dd, $J = 10.8$ Hz, 1H), 4.29 (dd, $J = 11.2$ Hz, 1H), 1.24 (s, 9H). Anal. Calcd for $\text{C}_{29}\text{H}_{28}\text{N}_4\text{O}_7$: C, 63.96; H, 5.18; N, 10.29. Found: C, 63.68; H, 5.50; N, 10.41.

4.3.8. Synthesis of 6 (TX-2037). Diisopropylcarbodiimide (ca. 164 mg/200 μL , 1.3 mmol) was added to a solution of (2*S*)-*p*-*tert*-butylphenoxy-1-(2-nitroimidazolyl)-2-propanol **20**⁷ (159.7 mg, 0.5 mmol), **10** (237.0 mg, 1 mmol), and 4-dimethylaminopyridine (18 mg, 0.1 mmol) in acetonitrile (5 mL) and the mixture was stirred under nitrogen at 30–45 °C for 24 h. It was then cooled, filtered, and the filtrate was evaporated to dryness. The residue of crude product mixture was dissolved in CH_2Cl_2 (20 mL) and ethyl acetate (10 mL), washed with 5% sodium bicarbonate and brine, dried (Na_2SO_4), and concentrated in vacuo. The crude product was purified by flash chromatography (ethyl acetate/hexane, 2:3) to afford (2*S*)-3-*p*-*tert*-butylphenoxy-1-(2-nitroimidazolyl)-2-propyl-4'-(trifluoroacetamido)benzoate, **23** (258 mg, 96.5%). Mp 179–180 °C; IR (KBr; cm^{-1}): 3337, 3123, 2974, 1717, 1605, 1541, 1493, 1365, 1253, 1199, 1157, 1103, 767, 735; ^1H NMR ($\text{C}_2\text{D}_6\text{SO}$): δ 11.55 (s, 1H), 7.92 (d, $J = 8.4$ Hz, 2H), 7.82 (d, $J = 8.8$ Hz, 2H), 7.66 (s, 1H), 7.08 (s, 1H), 5.46 (m, 1H), 4.90 (dd, $J = 7.2$ Hz, 1H), 4.65 (dd, $J = 9.2$ Hz, 1H), 3.65 (dd, $J = 7.4$ Hz, 2H), 1.19 (s, 9H).

Sodium borohydride (39.2 mg, 1.05 mmol) was added to a solution of **23** (243 mg, 0.45 mmol) in 10 mL of absolute ethanol, and the mixture was stirred for 24 h at room temperature after the reaction was quenched by dropwise addition of water (5 mL) and the volatile solvent was removed in vacuo. The remaining aqueous solution was then extracted with ethyl acetate and the organic layer was washed with brine, dried (Na_2SO_4), and concentrated in vacuo. The residue of crude product was purified by flash chromatography to afford (2*S*)-*p*-*tert*-butylphenoxy-1-(2-nitroimidazolyl)-2-propyl-4'-aminobenzoate, **26** (188.2 mg, 95.4%). Mp 110–111 °C; IR (KBr; cm^{-1}): 3348, 2969, 1701, 1625, 1602, 1514, 1489, 1364, 1268, 1171, 1100, 837, 768. ^1H NMR ($\text{C}_2\text{D}_6\text{SO}$): δ 11.55 (s, 1H), 7.92 (d, $J = 8.4$ Hz, 2H),

7.82 (d, $J = 8.8$ Hz, 2H), 7.66 (s, 1H), 7.08 (s, 1H), 5.46 (m, 1H), 4.90 (dd, $J = 7.2$ Hz, 1H), 4.65 (dd, $J = 9.2$ Hz, 1H), 3.65 (dd, $J = 7.4$ Hz, 2H), 1.19 (s, 9H). MS (EI) m/z : 438 (M^+).

A mixture of **17** (58.6 mg, 0.42 mmol), **26** (158.6 mg, 0.36 mmol), and EtOH (10 mL) was refluxed for 24 h and then was evaporated under aspirator vacuum. The residue was purified by silica gel column chromatography (silica gel 60 N, hexane/ethyl acetate, 3:2) to give yellow crystals of **6** (TX-2037, 153.9 mg, 78.5%), Mp 187–188 °C; $[\alpha]_D^{26} -68.4^\circ$ (c 0.98, $CHCl_3$), IR (KBr; cm^{-1}): 3424, 2966, 1719, 1661, 1602, 1489, 1365, 1266, 1104, 846, 764; 1H NMR (C_2D_6SO): δ 8.03 (d, $J = 11.6$ Hz, 1H), 7.85 (d, $J = 8.8$ Hz, 2H), 7.63 (d, $J = 8.8$ Hz, 2H), 7.29 (d, $J = 8.8$ Hz, 2H), 6.91 (d, $J = 8.8$ Hz, 2H), 7.69 (s, 1H), 7.10 (d, $J = 0.8$ Hz, 1H), 5.77 (m, 1H), 5.01 (d, $J = 11.6$ Hz, 1H), 4.83 (dd, $J = 9.2$ Hz, 1H), 4.36 (dd, $J = 11.6$ Hz, 1H), 4.29 (d, $J = 11.6$ Hz, 1H), 1.24 (s, 9H). Anal. Calcd for $C_{29}H_{28}N_4O_7$: C, 63.96; H, 5.18; N, 10.29. Found: C, 63.69; H, 5.41; N, 10.02.

4.4. Biological activities

4.4.1. Compounds. All compounds tested were dissolved in dimethylsulfoxide (DMSO) before treatment. Control experiments consisted of addition of DMSO (<0.5% or 1%) alone.

4.4.2. Hypoxic cytotoxicity. To estimate hypoxic cytotoxicity, cells were incubated under aerobic or hypoxic conditions in a suspension culture system. Monolayers of the cells in exponential growth were trypsinized, suspension cultures at a density of 2×10^6 cells/mL were prepared and 495 μ L of the suspension was set up in glass tubes. The drug solutions, 100-fold more concentrated, were added at a volume of 5 μ L to each tube. The glass tubes were stoppered with rubber caps perforated with a 22 G \times 1 1/4 in. needle to provide gas inlet and an 18 G \times 70 mm needle as an outlet. The tubes were shaken and flushed with humidified 5% CO_2 and 95% N_2 at room temperature at flow rates of 1.5–2.0 nl/min for 1 h. They were then allowed to stand for an additional 2 h, tightly stoppered. In the case of aerobic conditions, the tubes with loose caps were shaken and then left to stand at room temperature for the same period.

4.4.3. In vitro radiosensitization. The effects of radiosensitizers were measured under hypoxic conditions using EMT6/KU cells as described by Shibamoto¹² Briefly, cells were suspended in glass test tubes (2×10^6 cells/mL MEM containing drug) and the tubes were made hypoxic by purging with a gas mixture comprising 95% N_2 –5% CO_2 for 60 min. Tubes were then irradiated using 6 MV X-rays generated by a medical linear accelerator at a dose rate of 2.0 Gy/min. Immediately after irradiation, the cells were resuspended in MEM at appropriate concentrations and plated onto 6 cm tissue culture dishes. After 5–7 days of culture, the cells were plated in appropriate numbers to assay for colony-forming ability. The survival data were fitted with lines by the

least-squares method. The enhancement ratio (ER) values were determined from the ratio of radiation doses required to reduce the surviving fraction of the cells to 1%.

4.4.4. Clonogenic assay. The surviving cell fractions after drug treatment under hypoxic or aerobic conditions were determined in a colony formation assay. After treatment as described above, cells were trypsinized, diluted to a suitable density, and plated in a dish. The colonies obtained after 10 days were fixed with methanol and stained with 5% Giemsa solution. Visible colonies composed of more than 50 cells were counted as having grown from surviving cells. The plating efficiency (PE) was calculated by dividing the number of colonies by the number of cells seeded. The surviving cell fraction for the treatment at each drug concentration was calculated as PE treated/PE control. Drug potency was considered to be the concentration (μ M) that resulted in up to 10% clonogenic cell survival under hypoxia ($IC_{0.1}$). Values are the means of at least two independent experiments.

4.4.5. Endothelial cell proliferation assay. Rat lung endothelial (RLE) cells were provided by Dr. G.L. Nicolson, Texas M.D. Anderson Hospital, Houston, Texas, and maintained at exponential growth in spinner culture. MTT [3-(4,5-dimethyl-2-thiazolyl)-2,5-diphenyl-2H tetrazolium bromide] was purchased from Dojindo Laboratories (Kumamoto, Japan). Optical density was measured on a microplate reader (Bio-Rad model 450, Japan Bio-Rad Laboratories, Tokyo, Japan) using 570 nm filter with blanking at 700 nm. The MTT assay was performed by suspending the cells in Eagle's MEM containing 7% $NaHCO_3$ and 4.7% FCS (pH 7.4), then pouring 300 μ L into the wells of 48-well culture.

4.4.6. Chick embryo chorioallantoic membrane assay. Antiangiogenic activity was assayed using chick embryo chorioallantoic membrane (CAM) according to the method described by Oikawa.¹³ Using a 4-day-old chick embryo (Goto Hatchery, Inc., Japan) in a shell, 10 μ L of the sample mixed in 1% methyl cellulose/0.9% NaCl was applied into the ring put onto the surface of the CAM. After 48 h of exposure at 37.6 °C, a fat emulsion (Mitsubishi Pharma Corporation, Osaka, Japan) was injected into the CAM to visualize blood vessels clearly. Each experimental group included six eggs, and experiments were repeated more than three times. Angiogenic inhibition was indicated by the presence of a 3-mm-diameter avascular zone around the ring. An avascular zone around the ring of 3 mm diameter indicated angiogenic inhibition. Inhibition of angiogenesis (%) was calculated as (number of eggs showing at least 3 mm zone of inhibition)/(number of eggs used in each experimental group) \times 100.

4.4.7. MMP inhibition assays¹⁴. Progelatinase A (pro-MMP-2) and B (pro-MMP-9) from human Bowes melanoma cells and bovine arterial endothelial cells, respectively, were used. Proenzymes were activated immediately prior to use with 1 mM *p*-aminophenylmer-

curic acetate (APMA) for 1 h at 37 °C. For assay measurements, the inhibitor stock solutions (DMSO, 100 mM) were further diluted at various concentrations. Assay with MMP-2 was performed in Tricine 50 mM, pH 7.5, NaCl 200 mM, CaCl₂ 10 mM, DMSO 0.5% and assay with MMP-9 was performed in Tricine 50 mM, pH 7.5, NaCl 200 mM, CaCl₂ 10 mM, Brij 35 0.05%, ZnSO₄ 50 μM, and DMSO 0.5%. Generally, 190 μL of assay buffer containing activated enzyme and inhibitor solutions was incubated for 1 h at 25 °C. Ten microliters of the fluorogenic substrate DNP-Pro-Leu-Gly-Met-Trp-Ser-Arg-OH (Carbiochem) in DMSO (final concentration 200 μM) was added and incubated overnight at 37 °C. The hydrolysis was stopped with acetic acid and diluted ten times, then monitored fluorescence (excitation maximum 280 nm, emission maximum 360 nm) using F-2000 fluorescence spectrometer (Hitachi Co., Ltd). Control wells lack inhibitor. Percent of inhibition was calculated from control reactions without the inhibitor.

4.4.8. PTK inhibition assay.

4.4.8.1. Materials. [γ -³²P]ATP was purchased from NEN Research Products (Wilmington, DE, USA).

4.4.8.2. Assay for Flt-1¹⁵. v-src Transformed NIH3T3 cells were incubated for 10 min on ice in a hypotonic buffer (1 mM Hepes, pH 7, 4.5 mM MgCl₂, and 25 μg/mL each of the protease inhibitors antipain, leupeptin, and pepstatin A). The swollen cells were homogenized by vortexing for 2 min at room temperature. Following an increase of Hepes to 20 mM, the homogenate was centrifuged at 500g for 5 min to sediment nuclei. To this supernatant, addition was made to give a final concentration of 20 mM Hepes, pH 7.4, 10 mM MgCl₂, 0.1 mM Na₃VO₄, 10 mM β-glycerophosphate, 1 mM NaF, and 2.5 mg/mL protein, 1 μM phorbol myristate 13-acetate (PMA) and 20 μM cAMP. Protein kinase inhibitors were dissolved in DMSO and the final concentration of DMSO in the reaction mixture was 10% (v/v). The kinase reaction was initiated by addition of [γ -³²P]ATP (12.5 μM, 10 μCi), and the solution was incubated for 15 min at 25 °C. The reaction was terminated by the addition of SDS-PAGE sample buffer. The phosphorylated proteins were separated by SDS-PAGE (9% w/v gels). To detect PTK activity, the dried gels were further treated with 1 N KOH at 55 °C for 2 h. The results were visualized by autoradiography or Fuji Film Bio-image Analyzer BAS 2000. From the enzyme activity (% of control) as a function of drug concentration, the IC₅₀ value was estimated as the index of the enzyme inhibition of drug.

4.4.8.3. Assay for EGFR-K¹⁶. To measure EGF-K activity, A431 human epithelial carcinoma cells were solubilized and cell debris was removed. Cell lysate was incubated with or without EGF at 25 °C for 30 min, and the reaction was started by addition of [γ -³²P]ATP and incubated at 0 °C for 10 min. After the reaction was stopped, the mixture was washed. To estimate phosphorylation of the receptor, the ³²P radioactivity was measured with a scintillation counter.

4.4.9. Antitumor screening on HCC panel^{17,18}. Each of the test compounds was added to a microtiter plate 24 h after cancer cells were enclosed into it. After 48 h incubation, the amount of the cells was colorimetrically determined using sulforhodamine B as the reagent and the percentage of cell proliferation was calculated against the control. An HCC panel containing 39 cell lines was employed for screening tests, in which GI₅₀ (compound concentration necessary to suppress cell proliferation to 50% of the control), TGI (compound concentration necessary to suppress cell proliferation to the cell number at time zero), LC₅₀ (compound concentration necessary to reduce cell number of that at time zero) were evaluated at 10⁻⁴–10⁻⁸ M compound concentrations for each cell line.

Acknowledgments

This work was partially supported by Grant-in-Aid for Young Scientist (B) (No. 18790892) from the Ministry of Education, Culture, Sports, Science and Technology, Japan. The authors thank the Screening Committee of New Anticancer Agents supported by Grant-in-Aid for Scientific Research of Priority Area ‘Cancer’ from the Ministry of Education, Science, Sports, Culture and Technology, Japan for the antitumor screening data on HCC panel. We also thank DAISO Co., Ltd. (Osaka, Japan) for providing (*R*)- and (*S*)-epichlorohydrin. The authors thank Dr. Hiromu Nishitani, Mr. Yasuo Nishimoto, Mr. Taro Kishi, and the staff of Department of Radiology, School of Medicine, The University of Tokushima for generous help with the radiological experiments. The authors also thank Ms. Maki Nakamura, Ms. Kayoko Yamashita, Ms. Emiko Okayama, and the staff of our Faculty for measurement of NMR, MS, and elemental analysis. K. Kirk acknowledges support from the NIDDK intramural research program.

References and notes

- Hanahan, D.; Weinberg, R. A. *Cell* **2000**, *100*, 57.
- Folkman, J. *Annu. Rev. Med.* **2006**, *57*, 1.
- Folkman, J. *J. Pediatr. Surg.* **2007**, *42*, 1.
- Shweiki, D.; Itin, A.; Soffer, D.; Keshet, E. *Nature* **1992**, *359*, 843.
- Moeller, B. J.; Cao, Y.; Vujaskovic, Z.; Li, C. Y.; Haroon, Z. A.; Dewhirst, M. W. *Semin. Radiat. Oncol.* **2004**, *14*, 215.
- Pugh, C. W.; Ratcliffe, P. J. *Nat. Med.* **2003**, *9*, 677.
- Jin, C. Z.; Nagasawa, H.; Shimamura, M.; Uto, Y.; Inayama, S.; Takeuchi, Y.; Kirk, K. L.; Hori, H. *Bioorg. Med. Chem.* **2004**, *12*, 4917.
- Hori, H.; Nagasawa, H.; Uto, Y.; Ohkura, K.; Kirk, K. L.; Uehara, Y.; Shimamura, M. *Biochim. Biophys. Acta* **2004**, *1697*, 29.
- Frisch, M. J.; Trucks, G. W.; Schlegel, H. B.; Scuseria, G. E.; Robb, M. A.; Cheeseman, J. R.; Zakrzewski, V. G.; Montgomery, J. A., Jr.; Stratmann, R. E.; Burant, J. C., et al. *Gaussian 98, Revision A.11*; Gaussian, Inc.: Pittsburgh PA, 2001.
- O'Reilly, M. S. *Semin. Radiat. Oncol.* **2006**, *16*, 45.
- Murata, R.; Nishimura, Y.; Hiraoka, M. *Int. J. Radiat. Oncol. Biol. Phys.* **1997**, *37*, 1107.

12. Shibamoto, Y.; Ono, K.; Takahashi, H.; Kano, E.; Hori, H.; Shibata, T.; Inayama, S.; Abe, M. *Jpn. J. Cancer Res.* **1986**, *77*, 1027.
13. Oikawa, T.; Shimamura, M.; Ashino, H.; Nakamura, O.; Kanayasu, T.; Morita, I.; Murota, S. *J. Antibiot. (Tokyo)* **1992**, *45*, 1155.
14. Netzel-Arnett, S.; Mallya, S. K.; Nagase, H.; Birkedal-Hansen, H.; Van Wart, H. E. Continuously recording fluorescent assays optimized for five human matrix metalloproteinases. *Anal. Biochem.* **1991**, *195*, 86.
15. Fukuzawa, H.; Li, P. M.; Mizuno, S.; Uehara, Y. *Anal. Biochem.* **1993**, *212*, 106.
16. Murakami, Y.; Fukuzawa, H.; Mizuno, S.; Uehara, Y. *Biochem. J.* **1994**, *301*, 57.
17. Monks, A.; Scudiero, D.; Skehan, P.; Shoemaker, R.; Paull, K.; Vistica, D.; Hose, C.; Langley, J.; Cronise, P.; Wolff, A. V.; Goodrich, M. G.; Campbell, H.; Mayo, J.; Boyd, M. J. *Natl. Cancer Inst.* **1991**, *83*, 757.
18. Yanori, T. *Jpn J. Cancer Chemother.* **1997**, *24*, 129.